journal

J. Am. Ceram. Soc., 91 [7] 2321–2327 (2008)
DOI: 10.1111/j.1551-2916.2008.02428.x

Effect of Yttria on Interfacial Reactions Between Titanium Melt and Hot-Pressed Yttria/Zirconia Composites at 1700°C

Chien-Cheng Lin,*,† Yao-Wen Chang, and Kun-Lin Lin

Department of Materials Science and Engineering, National Chiao Tung University, Hsinchu 30050, Taiwan

Kun-Fung Lin

Materials and Electro-Optics Research Division, Chung-Shan Institute of Science Technology, Taoyuan 32546, Taiwan

Various Y_2O_3/ZrO_2 samples were fabricated by hot pressing, whereby Y_2O_3 was mutually dissolved or reacted with ZrO_2 as a solid solution or $Zr_3Y_4O_{12}$. Hot-pressed samples were allowed to react with Ti melt at 1700°C for 10 min in argon. Microstructural characterization was conducted using X-ray diffraction and analytical electron microscopy. The Y_2O_3/ZrO_2 samples became more stable with increasing Y_2O_3 because Y_2O_3 was hardly reacted and dissolved with Ti melt. The incorporation of more than 30 vol% Y_2O_3 could effectively suppress the reactions in the Ti side, where only a very small amount of α-Ti and β′-Ti was found. When ZrO_2 was dissolved into Ti on the zirconia side near the original interfaces, Y_2O_3 reprecipitated in the samples containing 30%–70 vol% Y_2O_3, because the solubility of Y_2O_3 in Ti was very low. In the region far from the original interface, α-Zr, Y_2O_3, and/or residual $Zr_3Y_4O_{12}$ were found in the samples containing more than 50 vol% Y_2O_3 and the amount of α-Zr decreased with increasing Y_2O_3.

I. Introduction

THE majority of ceramic materials seriously react with titanium and titanium alloys during casting, resulting in an α-casing and the deterioration of mechanical properties. Because no suitable ceramic crucible is available, titanium and titanium alloys are usually melted in a water-cooled copper crucible by consumable electrode vacuum arc melting (VAR) instead of vacuum induction melting (VIM). However, there are some drawbacks to the VAR process, including the high cost of the equipment, scrape recycle, and long cycle time. If a suitable crucible material were available, the VIM process would be feasible in industry. Furthermore, titanium castings need to be chemically milled in order to remove the reaction products on their surface. If the interfacial reactions between titanium and ceramic mold were well controlled, the chemical milling of the so-called α-casing would not be required. Therefore, determining how to control the interfacial reactions between titanium melt and some ceramic materials is of great interest.

Extensive studies have been carried out on the interfacial reactions between titanium melt and zirconia molds and/or crucibles in the last few decades.[1–8] Saha and Jacob[4] indicated that a brittle α-case was formed at the surface of titanium parts and thus adversely affected their mechanical properties. Weber and his coworkers[5,7] found a feather-like eutectic phase and blackened zirconia after titanium alloys reacted with a zirconia crucible. Zhu *et al.*[6] claimed that there were two distinct chemical reaction layers at the interface between titanium melt and zirconia after reaction at 1700°C. Holcombe and Serandos[9] stated that the composite crucible of W and Y_2O_3 revealed little contamination after reaction with titanium melt.

Recently, Lin and colleagues[10–16] have thoroughly investigated the interfacial reaction mechanisms between titanium (or titanium alloys) and 3Y–ZrO_2 using analytical transmission electron microscopy. The lamellar orthorhombic Ti_2ZrO and the ordered titanium suboxide (Ti_3O) were formed in α-Ti(Zr, O) at the interface between Ti melt and 3Y–ZrO_2 after reaction at 1750°C.[10] For the Ti/3Y–ZrO_2 diffusion couple, both lamellar orthorhombic Ti_2ZrO and spherical hexagonal Ti_2ZrO were found in α-Ti(Zr, O) after annealing at 1550°C.[11,13,14] In addition, the orientation relations of acicular α-Ti and β′-Ti were determined to be $[2\bar{1}\bar{1}0]_{\alpha-Ti}//[001]_{\beta'-Ti}$ and $(0001)_{\alpha-Ti}//(100)_{\beta'-Ti}$ in combination of $[2\bar{1}10]_{\alpha-Ti}//[021]_{\beta'-Ti}$ and $(0001)_{\alpha-Ti}//(1\bar{1}2)_{\beta'-Ti}$, respectively. Lin and Lin[12] also found intergranular α-Zr, twinned t'-ZrO_{2-x}, lenticular t-ZrO_{2-x}, and ordered c-ZrO_{2-x} on the zirconia side far from the interface between Ti and 3Y–ZrO_2 after annealing at 1550°C.

Various ratios of Y_2O_3/ZrO_2 samples were attempted in this study to achieve better control over the reactions on the titanium side as well as the ceramic side. The powder mixtures of Y_2O_3/ZrO_2 were hot pressed and then allowed to react with titanium melt at 1700°C for 10 min in argon. Various reaction layers at the interface between titanium melt and Y_2O_3/ZrO_2 samples were characterized using analytical scanning electron microscopy and analytical transmission electron microscopy. The effect of Y_2O_3 on the interfacial reactions between Ti melt and Y_2O_3/ZrO_2 samples will be elucidated in this study.

II. Experimental Procedure

The starting powders used were zirconia (>99.95 wt% ZrO_2+HfO_2 with HfO_2 accounting for approximately 2%–3% of this total, <0.002 wt% SiO_2, <0.002 wt% Al_2O_3, <0.005 wt% Fe_2O_3, <0.005 wt% TiO_2, <0.002 wt% CaO; 0.5 μm in average; Toyo Soda Mfg. Co., Tokyo, Japan), yttria (>99.9 wt% Y_2O_3 with trace rare earth oxides <0.001 wt% CeO_2, <0.001 wt% Pr_6O_{11}, <0.01 wt% Nd_2O_3, <0.003 wt% Sm_2O_3, <0.005 wt% Tb_4O_7, <0.005 wt% Dy_2O_3, <0.001 wt% CaO, <0.001 wt% Fe_2O_3 and other traces in balance; 0.5 μm in average; NYC Ltd., Fukuoka, Japan), and commercially pure titanium (with a nominal composition of 99.31 wt% Ti, 0.3 wt% Fe, 0.25 wt% O, 0.1 wt% C, 0.03 wt% N, 0.01 wt% H, 60–70 μm average in diameter, Alfa Aesar, Ward Hill, MA).

Powder mixtures with various Y_2O_3/ZrO_2 ratios were dispersed in the ethanol solvent. The pH of the suspension was adjusted to 11 by adding NH_4OH, and the suspension was ultrasonically vibrated for about 10 min (Model XL-2020, Sonicator, Heat Systems Inc., Farmingdale, NY). The suspension was

M. Rigaud—contributing editor

Manuscript No. 24082. Received December 10, 2007; approved February 17, 2008.
*Member, The American Ceramic Society.
Research supported by Chung-Shan Institute of Science Technology under Contract No. BV96D08P.
†Author to whom correspondence should be addressed. e-mail: chienlin@faculty.nctu.edu.tw

Table I. Designations, Compositions, Hot-Pressing Conditions, Relative Densities, and XRD Phases of Hot-Pressed Y_2O_3/ZrO_2 Samples

Specimens	Composition (vol%)	Composition (mol%)	Hot-pressing conditions	Relative densities	XRD phases
10Y90Z	10% Y_2O_3+90% ZrO_2	5% Y_2O_3+95% ZrO_2	1550°C/30 min/1 atm Ar	98.0%	*c*-ZrO_2, *t*-ZrO_2, *m*-ZrO_2
30Y70Z	30% Y_2O_3+70% ZrO_2	17% Y_2O_3+83% ZrO_2	1550°C/30 min/1 atm Ar	98.6%	*c*-ZrO_2
50Y50Z	50% Y_2O_3+50% ZrO_2	32% Y_2O_3+68% ZrO_2	1550°C/30 min/1 atm Ar	98.8%	$Zr_3Y_4O_{12}$
70Y30Z	70% Y_2O_3+30% ZrO_2	52% Y_2O_3+48% ZrO_2	1550°C/30 min/1 atm Ar	98.1%	Y_2O_3, $Zr_3Y_4O_{12}$
90Y10Z	90% Y_2O_3+10% ZrO_2	81% Y_2O_3+19% ZrO_2	1600°C/30 min/1 atm Ar	98.1%	Y_2O_3
100Y0Z	100% Y_2O_3	100% Y_2O_3	1600°C/30 min/1 atm Ar	98.3%	Y_2O_3

dried in an oven at 150°C, ground with an agate mortar and pestle, and then the mixtures were passed through 80 mesh. Samples with various Y_2O_3/ZrO_2 ratios were prepared by hot pressing in a graphite furnace at 1550°–1600°C for 30 min in an Ar atmosphere (Model HP50-MTG-7010, Thermal Technology Inc., Santa Rosa, CA). Oxygen-deficient zirconia was formed in the as hot-pressed samples. To avoid the inaccuracy, samples were annealed in air at 1300°C for 1 h so that stoichiometric zirconia was obtained.

The hot press conditions, compositions, relative densities, and designations of Y_2O_3/ZrO_2 samples are listed in Table I. The Y_2O_3/ZrO_2 samples contained 10, 30, 50, 70, 90, and 100 vol% Y_2O_3, respectively, and were balanced with ZrO_2. The sample consisting of 10 vol% Y_2O_3 and 90 vol% ZrO_2 was designated as 10Y90Z, and so on. The apparent densities of all Y_2O_3/ZrO_2 powder mixtures were measured using gas pycnometry with 99.99% pure helium (Model MultiVolume Pycnometer 1305, Micromeritics, Norcross, GA). The bulk densities of the hot-pressed Y_2O_3/ZrO_2 samples were determined by the Archimedes method using water as an immersion medium. For a nonporous powder, the apparent density approximates the true density and can be used as the reference point in calculating the percentage of the theoretic density of a hot-pressed body. The relative densities of the hot-pressed samples were calculated as follows: relative density = (bulk density/apparent density) $\times$ 100%.

Hot-pressed samples were cut and machined to dimensions of about 10 mm $\times$ 10 mm $\times$ 5 mm. A bulk specimen was vertically placed into the zirconia crucible, and then tightly packed with commercially pure titanium powder. The crucible was put in an electric resistance furnace (Model No. 4156, Centorr Inc., Nashua, New Hampshire, UK) with tungsten mesh heating elements. The chamber was evacuated to 10^{-4} torr and then refilled with argon. The cycle of evacuation and purging with argon was repeated three times. The temperature was increased to 1700°C at a heating rate of 10°C/min, held at 1700°C for 10 min and then cooled to room temperature in the furnace. The bulk specimen was fully immersed in the titanium melt above the melting point of titanium (1668°C), resulting in an interfacial reaction between Ti and Y_2O_3/ZrO_2 composites.

The phase identification of Ti and Y_2O_3/ZrO_2 samples was performed using an X-ray diffractometer (XRD, Model MXP18, Mac Science, Yokohama, Japan). The operating conditions of X-ray diffraction were Cu$K\alpha$ radition at 50 kV and 150 mA, and a scanning rate of 2° /min.

A scanning electron microscope (SEM, Model JSM 6500F, JEOL Ltd., Tokyo, Japan) was used for microstructural observation on the interfaces between Ti and various Y_2O_3/ZrO_2 samples. Cross-sectional SEM specimens were cut and ground using standard procedures and finally polished using diamond pastes of 6, 3, and 1 μm in sequence.

The compositions of various phases in the reaction layers were measured by an electron probe microanalyzer (EPMA, JXA-8800M, JEOL Ltd., Tokyo, Japan) with an atomic number, absorption, and fluorescence correction (ZAF) program.[17] The operating conditions for EPMA were as follows: the accelerating voltage was 15 kV, the probe current was 1.5×10^{-8} A, and the beam diameter was 1 μm.

The interfacial microstructures were also characterized using a transmission electron microscope (TEM, Model Tecnai 20, Philips, Eindhoven, Holland) equipped with an energy-dispersive X-ray spectrometer (EDS, Model ISIS 300, Oxford Instrument Inc., London, UK). Cross-sectional TEM specimens were cut and then ground down to ~80 μm with a diamond matted disk, polished with diamond pastes of 6, 3, and 1 μm in sequence, and dimpled to a thickness of 50 μm. Finally the TEM specimens were ion milled by a precision ion miller (Model 691, Gatan Inc., Pleasanton, CA). Quantitative analyses of individual phases in the reaction layers were conducted by the Cliff–Lorimer standardless technique.[18]

III. Results and Discussion

(1) XRD Analyses

Figure 1 shows the X-ray diffraction spectra of various Y_2O_3/ZrO_2 samples as well as pure Y_2O_3 after hot pressing. These spectra were arranged for Y_2O_3, 90Y10Z, 70Y30Z, 50Y50Z, 30Y70Z, and 10Y90Z, respectively, in a sequence from top to bottom. X-ray phases of these hot-pressed Y_2O_3/ZrO_2 samples are summarized in Table I. In the hot-pressed 90Y10Z, all of the zirconia was dissolved in yttria such that only cubic Y_2O_3 was detected. The hot-pressed 70Y30Z consisted of rhombohedral $Zr_3Y_4O_{12}$ and cubic Y_2O_3, while the XRD spectrum of the hot-pressed 50Y50Z showed only rhombohedral $Zr_3Y_4O_{12}$ peaks.[19] As for the hot-pressed 30Y70Z, only the cubic ZrO_2 phase was detected because all of the Y_2O_3 went into solid solution in zirconia. In other words, the cubic ZrO_2 was fully stabilized in 30Y70Z. However, *c*-ZrO_2, *t*-ZrO_2, and *m*-ZrO_2 were found in 10Y90Z or in partially stabilized ZrO_2. In general, Y_2O_3 was mutually dissolved or reacted with ZrO_2 as a solid solution or $Zr_3Y_4O_{12}$ in hot-pressed Y_2O_3/ZrO_2 samples. Pascual and Durán[19] found Y_6ZrO_{11} after sintering at 2000°C for 3 h and subsequent prolonged annealing. However, Y_6ZrO_{11} was not

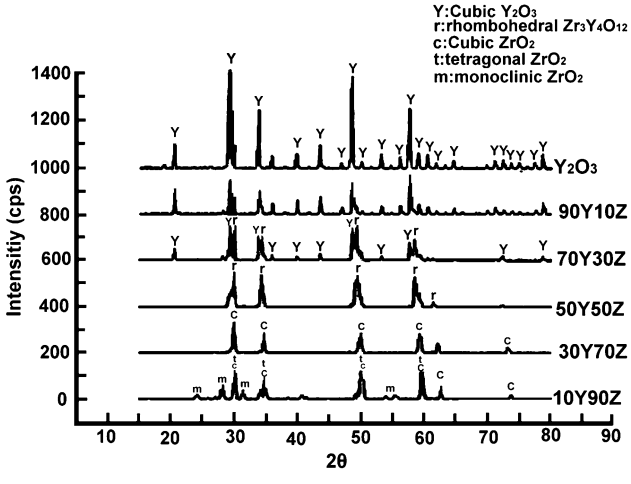

Fig. 1. X-ray diffraction spectra of as hot-pressed Y_2O_3/ZrO_2 samples.

found in this study because the equilibrium was probably not established.

(2) SEM and TEM Analyses

Figures 2(a)–(f) display backscattered electron images of cross-sections normal to the interfaces of Ti and various Y_2O_3/ZrO_2 samples after reaction at 1700°C for 10 min. Titanium is shown to the left of the micrograph, while zirconia is on the right-hand side. Arrows indicate the original interfaces of Ti and individual Y_2O_3/ZrO_2 samples. The original interfaces were deliberately located according to the characteristic $K\alpha$ X-ray maps of yttrium (not shown), which was relatively immobile with respect to Zr, O, Ti, etc. The large pores in the ceramic side, as shown in Figs. 2(a) and (b), were attributed to the Kirkendall effect because Zr and O diffused to the titanium side more rapidly than Ti diffused to the zirconia side.

Figure 2 indicates that extensive reactions took place at the interface between Ti and 10Y90Z. It was previously reported that needle-like α-Ti and some lamellar phases were usually found in the titanium side because of the interfacial reactions between Ti and ZrO_2.[10,11,13,14] However, only a limited reaction took place on the titanium side at the interface between Ti and those samples containing more than 30 vol% Y_2O_3, while

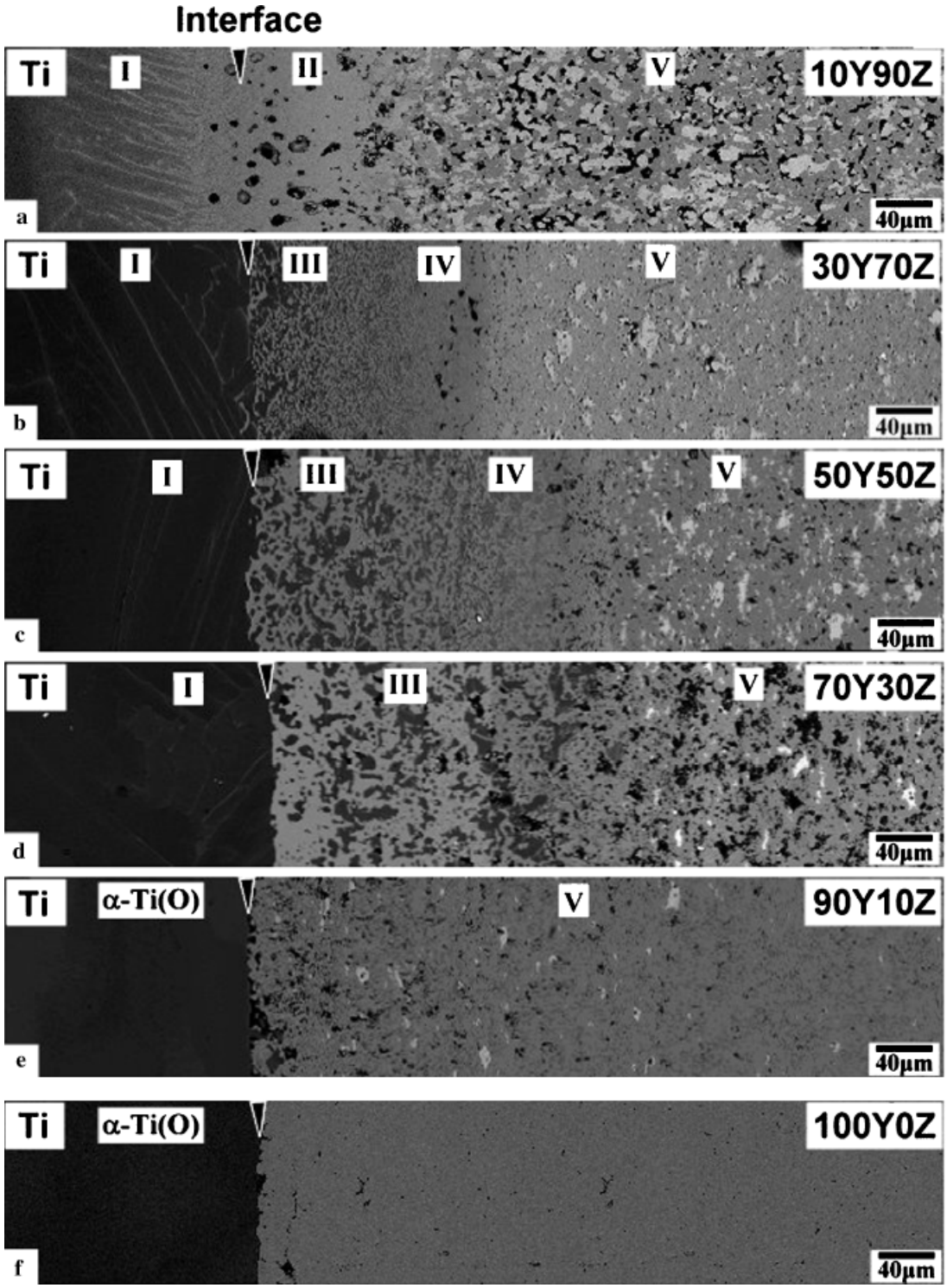

Fig. 2. (a)–(f) Backscattered electron images of the cross section between Ti and Y_2O_3/ZrO_2 samples after reaction at 1700°C for 10 min. Arrows indicate the original interfaces between Ti and Y_2O_3/ZrO_2 samples.

90Y10Z and pure Y_2O_3 reacted minimally with Ti melt. This indicated that interfacial reactions were effectively suppressed in those samples containing more than 30 vol% Y_2O_3. This fact plays an important role in the engineering aspect of Ti castings such that a controlled interfacial reaction results in a lower amount of α-casing and thus better mechanical properties. Even though the system became more stable with increasing Y_2O_3, several reaction layers were found on the zirconia side after interfacial reactions between Ti and various Y_2O_3/ZrO_2 samples. Microstructures of the reaction layers at the interface between Ti and various Y_2O_3/ZrO_2 samples were characterized using SEM/EDS and TEM/EDS and the results are listed in Table II. The details will be described below.

(A) Reaction Layer "I" on the Metal Side: The reaction layer "I" was observed on the metal side of the interfaces between Ti and Y_2O_3/ZrO_2 samples containing less than 70 vol% Y_2O_3 as shown in Figs. 2(a)–(d). An α-Ti phase with a small amount of oxygen in solid solution was to the left of reaction layer "I." The reaction layer "I" consisted of β′-Ti(Zr, O) and/or acicular α-Ti(Zr, O) in the α-Ti matrix. A clear comparison could be made with Fig. 3, displaying the backscattered electron images of the reaction layer "I" in 10Y90Z, 30Y70Z, and 50Y50Z, respectively, at higher magnification. As shown in Fig. 3(a) together with Fig. 2(a), a large amount of β′-Ti(Zr, O) and acicular α-Ti(Zr, O) ws precipitated in the α-Ti matrix at the interface between Ti and 10Y90Z. However, a relatively small amount of β′-Ti and acicular α-Ti existed at the interface between Ti and 30Y70Z [Fig. 3(b)] and only very few β′-Ti at the interface between Ti and 50Y50Z [Fig. 3(c)]. For comparison, several reaction layers consisting of α-Ti(Zr, O), β′-Ti(Zr, O), and Ti_2ZrO were found in the diffusion couple of Ti and 3Y–ZrO_2 after reactions ranging from 1400° to 1550°C.[11,13,14]

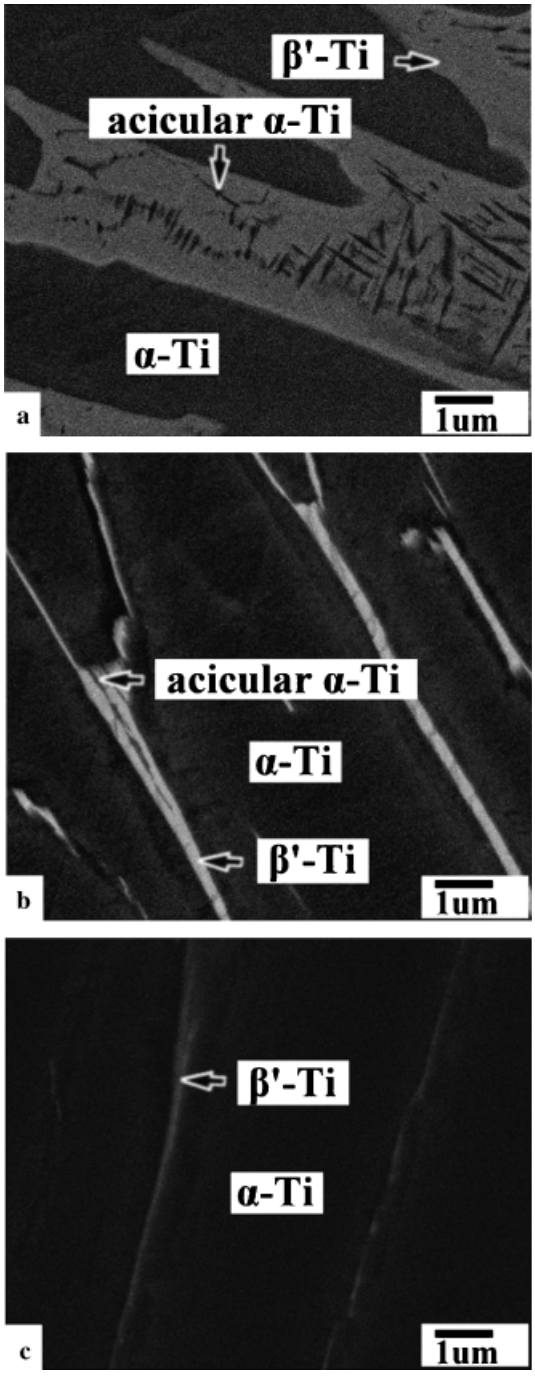

Fig. 3. Backscattered electron images of reaction layer "I" in the titanium side at the interface between (a) Ti and 10Y90Z, (b) Ti and 30Y70Z, and (c) Ti and 50Y50Z after reaction at 1700°C for 10 min.

(B) Reaction Layer "II" on the Ceramic Side: Figure 4 shows the backscattered electron images of reaction layers "II" on the outermost ceramic side of Ti/10Y90Z after reaction at 1700°C for 10 min. β′-Ti (bright), acicular α-Ti (dark), and spherical c-ZrO_{2-x} coexisted in reaction layer "II" at the interface between Ti and 10Y90Z, where zirconia was extensively dissolved in titanium. Based on EPMA results, β′-Ti in reaction layer "II" consisted of 43.98 at.% Ti, 25.97 at.% Zr, and 30.05 at.% O, indicating that β′-Ti was stabilized by dissolving a significant amount of Zr. Concurrently, zirconia was retained as a cubic phase because it dissolved as high as 10.7 at.% Y as a stabilizer. This was consistent with the results found by Zhu *et al.*,[6] indicating that Y was retained in cubic zirconia, when Y_2O_3-stabilized zirconia was reacted with molten titanium. Lin and Lin[13,14] also indicated a two-phase region of β′-Ti and c-ZrO_2 in the Ti/3Y–ZrO_2 diffusion couple after reaction at 1550°C. It was believed that reaction layer "II" was formed because titanium melt infiltrated along the grain boundaries of 10Y90Z.

(C) Reaction Layers "III" and "IV" on the Ceramic Side: Microstructures of reaction layers "III" and "IV" at the interface between Ti and 30Y70Z were very different from those of the corresponding reaction layers previously found in the Ti/ZrO_2 diffusion couples.[13,14] Figure 5 demonstrates microstructural variations in reaction layers "III" and "IV," as well as the observation that reaction layer "III" consisted of α-Ti, acicular α-Ti, β′-Ti, and Y_2O_3 at the interface between Ti and 30Y70Z after reaction at 1700°C for 10 min. Acicular α-Ti was found in β′-Ti as indicated by the arrow in Fig. 5(a). Based on EPMA analyses, β′-Ti consisted of 57.92 at.% Ti, 20.31 at.% Zr, and 21.77 at.% O, while the composition of acicular α-Ti was measured as 52.63 at.% Ti, 13.86 at.% Zr, and 33.51 at.% O. Because β′-Ti had a larger Zr/O ratio than α-Ti, β′-Ti looked brighter than α-Ti in backscattered electron images. The com-

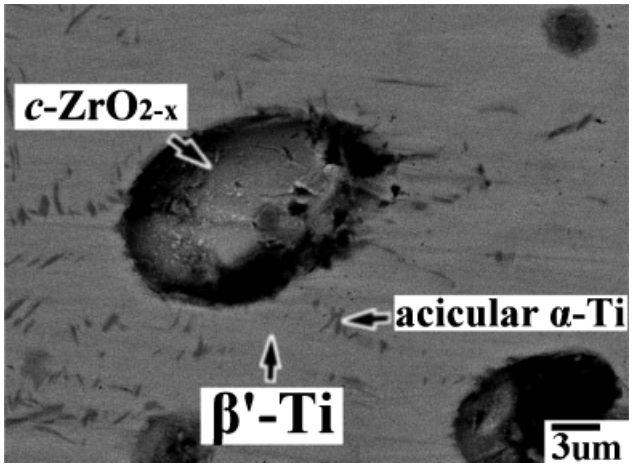

Fig. 4. Backscattered electron image of reaction layer "II" at the interface between Ti and 10Y90Z after reaction at 1700°C for 10 min.

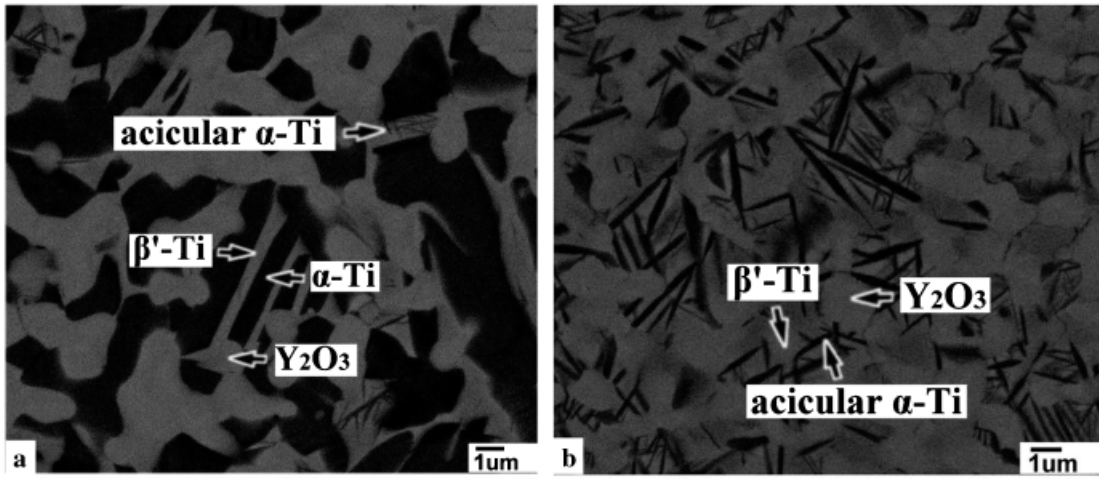

Fig. 5. Backscattered electron images of (a) reaction layer "III" and (b) reaction layer "IV" at the interface between Ti and 30Y70Z after reaction at 1700°C for 10 min.

position of Y_2O_3 was measured as 5.93 at.% Ti, 34.51 at.% Y, 4.50 at.% Zr, and 55.06 at.% O, indicating a significant amount of Ti and Zr in solid solution.

Figure 5(b) displays the backscattered electron image of reaction layer "IV" at the interface between Ti and 30Y70Z after reaction at 1700°C for 10 min. Reaction layer "IV" in 30Y70Z consisted of acicular α-Ti, β′-Ti, and Y_2O_3. β′-Ti was Ti with zirconium and oxygen in solid solution, consisting of 52.9 at.% Ti, 27.6 at.% Zr, and 19.5 at.% O, while Y_2O_3 was composed of 3.0 at.% Ti, 37.1 at.% Y, 1.6 at.% Zr, and 58.3 at.% O, respectively. All compositions were measured using EPMA. Reaction layer "IV" dissolved a larger amount of Zr in Ti than reaction layer "III." It was thus inferred that reaction layer "IV" was likely to be stabilized as the β phase at 1700°C because Zr is an effective β-stabilizer. During cooling, β-Ti was transformed into β′-Ti accompanied by the precipitation of acicular α-Ti in the β′-Ti matrix.[20]

As 30Y70Z reacted with Ti melt, a large amount of Zr and O from 30Y70Z was dissolved in titanium, giving rise to the formation of Y_2O_3 due to the very limited solubility of yttrium in titanium. The precipitation of Y_2O_3 was increased with increasing Y_2O_3/ZrO_2 ratio. It was noted that no interfacial reactions were found at the interface between Ti and 90Y10Z after reaction at 1700°C for 10 min. It was concluded that increasing Y_2O_3 content was useful for better controlling the interfacial reactions.

In the case of the Ti/ZrO_2 diffusion couple, Lin and Lin[13,14] found previously that acicular α-Ti precipitated in the β′-Ti matrix of the titanium side . However, acicular α-Ti and the β′-Ti matrix existed in reaction layers "III" and "IV" of the ceramic side in this study. This was attributed to the infiltration of titanium melt into the ceramic side, whereby reactions between Ti and ZrO_2 took place. In contrast, the faster diffusion of O and Zr into the titanium side led to the formation of the (α-Ti+β′-Ti) layers in the Ti–ZrO_2 diffusion couple.

Figure 6(a) shows the bright field image of the cross-section normal to the interface of Ti and 30Y70Z after reaction at 1700°C for 10 min. The orientation relationship of acicular α-Ti and β′-Ti was identified to be $[2\bar{1}\bar{1}0]_{\alpha-Ti}//[001]_{\beta'-Ti}$ and $(0001)_{\alpha-Ti}//(100)_{\beta'-Ti}$ as indicated in Fig. 6(b), in agreement with the results presented by Lin and Lin.[13,14] The selected-area diffraction pattern depicted in Fig. 6(c) indicated the existence of cubic Y_2O_3 in reaction layer "IV."

Microstructural evolution of reaction layer "III" at the interface between Ti and 30Y70Z at 1700°C is schematically displayed in Fig. 7(a). Upon heating to 1700°C, titanium melt infiltrated and dissolved a large amount of Zr and O, resulting in the formation of a two-phase (α-Ti+β-Ti) layer. Because the solubility of yttrium in titanium is quite limited, it remained as Y_2O_3 [the center of Fig. 7(a)]. During cooling, cubic β-Ti was transformed into orthorhombic β′-Ti, where a small amount of acicular α-Ti was precipitated [the right of Fig. 7(a)]. Figure 7(b) displays a proposed model of microstructural evolution in reaction layer "IV" at the interface between Ti and 30Y70Z at 1700°C. Because less titanium melt infiltrated into reaction layer "IV," Ti dissolved more concentrated Zr and O and existed as β-Ti during heating at 1700°C. As the solubility of yttrium in titanium was quite limited, Y_2O_3 was retained in the matrix of β-Ti at high temperatures [the center of Fig. 7(b)]. During cooling, the cubic β-Ti was transformed into orthorhombic β′-Ti where acicular α-Ti was precipitated in this reaction layer [Fig. 7(b), right side].

(D) Reaction Layer "V" on the Ceramic Side: Figures 8(a)–(c) show the bright field images of reaction layer "V" on the

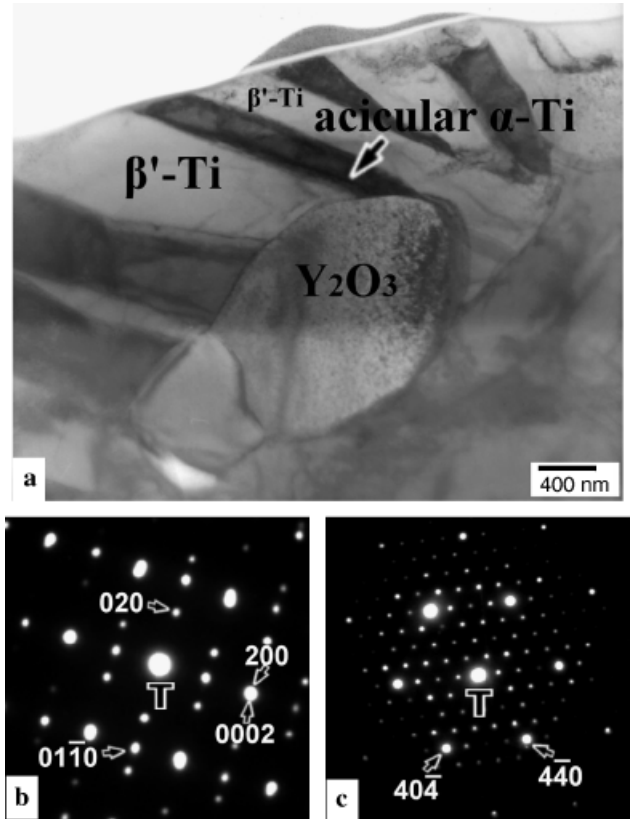

Fig. 6. (a) Bright-field image of reaction layer "IV" at the interface between Ti and 30Y70Z after reaction at 1700°C for 10 min; (b) selected-area diffraction patterns of acicular α-Ti and the matrix β′-Ti; (c) a selected-area diffraction pattern of Y_2O_3 with the zone axis [111].

ceramic side far from the original interface of Ti and 10Y90Z, 30Y70Z, and 50Y50Z, respectively, after reaction at 1700°C for 10 min. Figure 8(a) demonstrates that *t*-ZrO_{2-x} with two variants was precipitated in *c*-ZrO_{2-x} at the interface between Ti and 10Y90Z after reaction at 1700°C for 10 min. Because Y_2O_3 was completely retained in ZrO_2, no free Y_2O_3 was found in 10Y90Z. Figure 8(b) shows that several α-Zr particles were embedded in *c*-ZrO_{2-x} in reaction layer "V" of 30Y70Z after reaction at 1700°C for 10 min. The composition of α-Zr was measured using EPMA, indicating that it contained 2.43 at.% Y, 69.14 at.% Zr, and 28.43 at.% O. Figure 8(c) shows the bright field image of reaction layer "V" in 50Y50Z after reaction at 1700°C for 10 min. Residual $Zr_3Y_4O_{12}$ was found and its crystal structure was identified to be rhombohedral based on the inset selected-area diffraction pattern, as shown in the upper right corner of Fig. 8(c). Figure 8(d) shows an EDS spectrum of this ternary compound. The average composition was calculated from six measurements to be 15.88 at.% Zr, 22.08 at.% Y, and 62.04 at.% O in correspondence withthe composition of $Zr_3Y_4O_{12}$.

It was believed that the oxidation–reduction reaction rather than dissolution was the predominant reaction mechanism in reaction layer "V." Dissolution did not play a significant role, as the titanium was not detected by EDS in reaction layer "V." The oxidation–reduction reaction between Ti and ZrO_2 resulted in the formation of metastable oxygen-deficient zirconia (ZrO_{2-x}). It was inferred that α-Zr precipitated from the supersaturated *c*-ZrO_{2-x}, accompanied with an increasing O/Zr ratio in ZrO_{2-x}[21]. Furthermore, the amount of α-Zr decreased with increasing amounts of Y_2O_3 because Y_2O_3 could effectively suppress the reaction between Ti and ZrO_2.

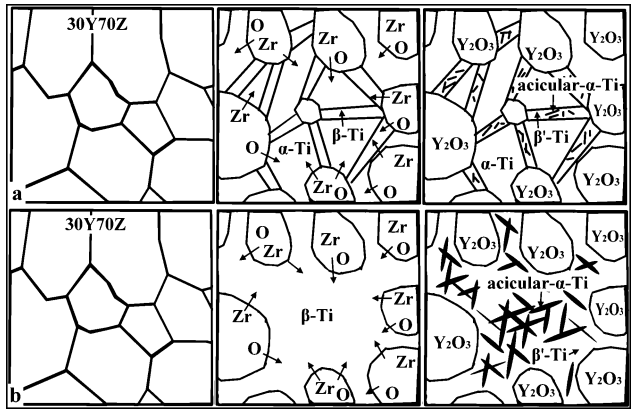

Fig. 7. Schematic diagrams showing the microstructural evolution of (a) reaction layer "III" and (b) reaction layer "IV" at the interface between Ti and 30Y70Z at various stages.

(3) A General Discription of Interfacial Reaction Layers

According to the above discussion, the reaction layers were formed at the interface between titanium and yttria/zirconia samples after reaction at 1700°C for 10 min (summarized in Table II). Briefly speaking, extensive reactions occurred at the interface between Ti and 10Y90Z as previous studies indicated.[11-14] However, interfacial reactions were effectively suppressed by incorporating more than 30 vol% Y_2O_3. The interfaces were increasingly stable with the amount of Y_2O_3 because Y_2O_3 functioned as a reaction barrier phase. On the metal

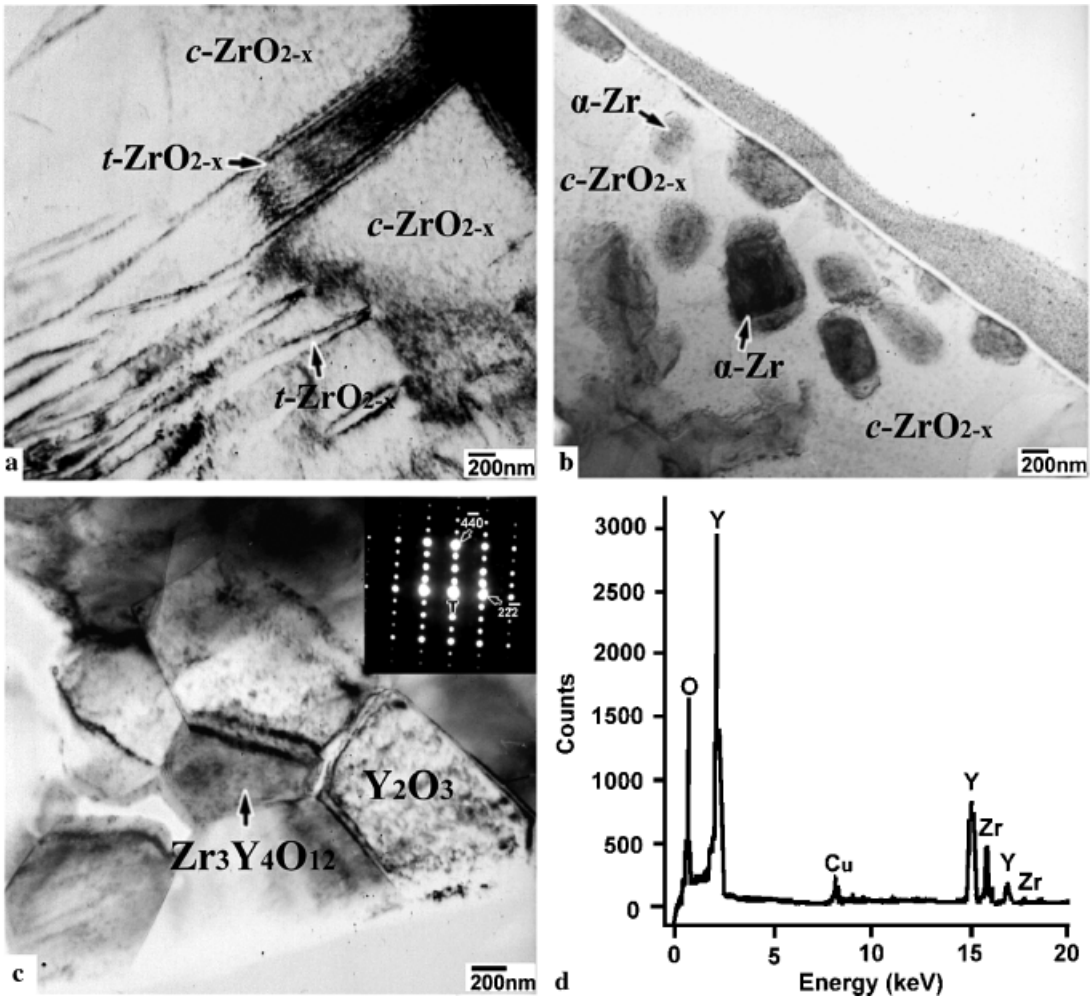

Fig. 8. Bright-field images of reaction layer "V" in the zirconia side far away from the interface between (a) Ti and 10Y90Z, (b) Ti and 30Y70Z, and (c) Ti and 50Y50Z after reaction at 1700°C for 10 min. The inset in the upper right-hand corner of Fig. 8(c) is the selected-area diffraction pattern of $Zr_3Y_4O_{12}$ with the zone axis [112]; (d) an energy-dispersive spectrum of $Zr_3Y_4O_{12}$.

Table II. Reaction Layers Formed at the Interfaces of Ti and Y_2O_3/ZrO_2 Samples After Reaction at 1700°C/10 min

Specimens	Mol% Y_2O_3	Interface reaction layers and phases: Ti side		Ceramic side		Reaction layer "V" in the ceramic side
10Y90Z	5	I	α-Ti, β′-Ti+acicular α-Ti	II	β′-Ti+acicular α-Ti, c-ZrO_{2-x}	*c*-ZrO_{2-x}, *t*-ZrO_{2-x}, α-Zr
30Y70Z	17	I	α-Ti, β′-Ti+acicular α-Ti	III	Y_2O_3, α-Ti, β′-Ti+acicular α-Ti	*c*-ZrO_{2-x}, α-Zr
				IV	Y_2O_3, β′-Ti+acicular α-Ti	
50Y50Z	32	I	α-Ti, β′-Ti	III	Y_2O_3,α-Ti, β′-Ti+acicular α-Ti	Y_2O_3, $Zr_3Y_4O_{12}$, α-Zr
				IV	Y_2O_3, β′-Ti+acicular α-Ti	
70Y30Z	52	I	α-Ti, β′-Ti	III	Y_2O_3, α-Ti, β′-Ti+acicular α-Ti	Y_2O_3, α-Zr
90Y10Z	81	Insignificant interfacial reaction				Y_2O_3, α-Zr
100Y0Z	100	Insignificant interfacial reaction				Y_2O_3

side, β′-Ti and acicular α-Ti were observed in the α-Ti matrix of reaction layer "I" after Ti reacted with 10Y90Z or 30Y70Z, although only a small amount of β′-Ti was found in the α-Ti matrix of reaction layer "I" for the cases of 50Y50Z and 70Y30Z. Furthermore, no reaction layer "I" was formed for the cases of 90Y10Z and pure Y_2O_3. In the outermost ceramic region, β′-Ti and α-Ti were found along with *c*-ZrO_{2-x} in reaction layer "II" of 10Y90Z, while β′-Ti and α-Ti were found along with Y_2O_3 in reaction layers "III" and "IV" of 30Y70Z, 50Y50Z, and 70Y30Z. Free Y_2O_3 existed in reaction layers "III" and "IV" due to a very limited solubility of Y_2O_3 in Ti when ZrO_2 was completely dissolved in Ti. On the ceramic side far from the original interface, dense α-Zr was formed in addition to residual ZrO_2 in reaction layer "V" of 10Y90Z and 30Y70Z, where α-Zr was excluded from metastable *c*-ZrO_{2-x}. However, α-Zr was formed in reaction layer "V" of 70Y30Z and 90Y10Z, because oxygen in ZrO_2 was extracted by Ti through the oxidation–reduction mechanism. The amount of α-Zr decreased with increasing amounts of Y_2O_3. Although Y_2O_3 was dissolved into ZrO_2 as a solid solution or reacted with ZrO_2 as $Zr_3Y_4O_{12}$ during hot pressing, Y_2O_3 was reprecipitated, due to the oxidation–reduction mechanism and strong affinity of O and Zr to Ti, in 50Y50Z and 70Y30Z after reaction at 1700°C for 10 min. It was also noted that some $Zr_3Y_4O_{12}$ grains were retained in 50Y50Z after reaction at 1700°C for 10 min.

IV. Conclusions

(1) The incorporation of more than 30 vol% Y_2O_3 significantly suppressed reactions at the interfaces between Ti and various Y_2O_3/ZrO_2 samples. In contrast, an extensive reaction occurred at the interface between Ti and 10Y90Z (or a partially stabilized ZrO_2) as mentioned previously.

(2) On the metal side, β′-Ti and acicular α-Ti were observed in the α-Ti matrix after Ti melt reacted with 10Y90Z or 30Y70Z at 1700°C for 10 min. However, only a very small amount of β′-Ti was found in the α-Ti matrix after Ti reacted with 50Y50Z or 70Y30Z. Ti was almost kept intact after reaction with 90Y10Z or Y_2O_3 at 1700°C for 10 min.

(3) After reaction at 1700°C for 10 min, β′-Ti, α-Ti and *c*-ZrO_{2-x} were found in the outermost region of 10Y90Z, while β′-Ti, α-Ti and Y_2O_3 existed in the outermost region of 30Y70Z, 50Y50Z, and 70Y30Z. The formation of Y_2O_3 in this region was caused by the extensive dissolution of ZrO_2 in Ti together with a very limited solubility of Y_2O_3.

(4) Dense α-Zr was formed along with residual ZrO_2 (cubic and/or tetragonal) or Y_2O_3 far from the original interface after reaction with Ti at 1700°C for 10 min. The amount of α-Zr decreased with increasing amounts of Y_2O_3.

(5) Y_2O_3, existing as a solid solution or $Zr_3Y_4O_{12}$ after hot pressing, was reprecipitated in 50Y50Z and 70Y30Z far from the original interface after reaction at 1700°C for 10 min. This was due to the oxidation–reduction reaction and the strong Ti affinity of O and Zr.

(6) Some $Zr_3Y_4O_{12}$ grains were retained in the sample containing 50 vol% Y_2O_3 after reaction at 1700°C for 10 min.

Acknowledgments

The authors would like to thank Mr. Wen-Shao Liao at the Department of Material Sciences and Engineering in National Chiao Tung University, Hsinchu, Taiwan, for preparing the SEM specimens.

References

[1]A. I. Kahveci and G. E. Welsch, "Effect of Oxygen on the Hardness and Alpha/Beta Phase Ration of Ti–6Al–4V Alloy," *Scr. Metall.*, **20** [9] 1287–90 (1986).
[2]K. I. Suzuki, S. Watakabe, and K. Nishikawa, "Stability of Refractory Oxides for Mold Material of Ti–6Al–4V Alloy Precision Casting," *J. Jpn. Inst. Met.*, **60** [8] 734–43 (1996).
[3]G. Welsch and W. Bunk, "Deformation Modes of the Alpha-Phase of Ti–6Ai–4V as a Function of Oxygen Concentration and Aging Temperature," *Metall. Trans. A*, **13A** [5] 889–99 (1982).
[4]R. L. Saha and K. T. Jacob, "Casting of Titanium and its Alloy," *Def. Sci.*, **36** [2] 121–41 (1986).
[5]B. C. Weber, H. J. Garrett, F. A. Mauer, and M. A. Schwartz, "Observations on the Stabilization of Zirconia," *J. Am. Ceram. Soc.*, **39** [6] 197–07 (1956).
[6]J. Zhu, A. Kamiya, T. Yamada, W. Shi, K. Naganuma, and K. Mukai, "Surface Tension, Wettability and Reactivity of Molten Titanium in Ti/Yttria-Stabilized Zirconia System," *Mater. Sci. Eng. A*, **327**, 117–27 (2002).
[7]B. C. Weber, W. M. Thompson, H. O. Bielstein, and M. A. Schwartz, "Ceramic Crucible for Melting Titanium," *J. Am. Ceram. Soc.*, **40** [11] 363–73 (1957).
[8]G. Economos and W. D. Kingery, "Metal–Ceramic Interactions: II, Metal Oxide Interfacial Reactions at Elevated Temperatures," *J. Am. Ceram. Soc.*, **36** [12] 403–9 (1953).
[9]C. E. Holcombe and T. R. Serandos, "Consideration of Yttria for Vacuum Induction Melting of Titanium," *Metall. Trans.*, **14B** [9] 497–8 (1983).
[10]K. F. Lin and C. C. Lin, "Transmission Electron Microscope Investigation of the Interface between Titanium and Zirconia," *J. Am. Ceram. Soc.*, **82** [11] 3179–85 (1999).
[11]K. L. Lin and C. C. Lin, "Ti_2ZrO Phases Formed in the Titanium and Zirconia Interface after Reaction at 1550°C," *J. Am. Ceram. Soc.*, **88** [5] 1268–72 (2005).
[12]K. L. Lin and C. C. Lin, "Zirconia-Related Phases in the Zirconia/Titanium Diffusion Couple after Annealing at 1100° to 1550°C," *J. Am. Ceram. Soc.*, **88** [10] 2928–34 (2005).
[13]K. L. Lin and C. C. Lin, "Microstructural Evolution and Formation Mechanism of the Interface Between Titanium and Zirconia Annealed at 1550°C," *J. Am. Ceram. Soc.*, **89** [4] 1400–8 (2006).
[14]K. L. Lin and C. C. Lin, "Effects of Annealing Temperature on Microstructural Development at the Interface Between Zirconia and Titanium," *J. Am. Ceram. Soc.*, **90** [3] 893–9 (2007).
[15]K. F. Lin and C. C. Lin, "Interfacial Reactions between Zirconia and Titanium," *Scr. Metall.*, **39** [10] 1333–8 (1998).
[16]K. F. Lin and C. C. Lin, "Interfacial Reactions between Ti–6Al–4V Alloy and Zirconia Mold During Casting," *J. Mater. Sci.*, **34**, 5899–906 (1999).
[17]J. I. Goldstein, *Scanning Electron Microscopy and X-ray Microanalysis*, 2nd edition, Plenum Press, New York, 1992.
[18]G. Cliff and G. W. Lorimer, "The Quantitative Analysis of Thin Specimens," *J. Microsc.*, **130** [3] 203–7 (1975).
[19]C. Pascual and P. Durán, "Subsolidus Phase Equilibria and Ordering in the System ZrO_2–Y_2O_3," *J. Am. Ceram. Soc.*, **66** [1] 23–7 (1983).
[20]R. F. Domagala, S. R. Lyon, and R. Ruh, "The Pseudobinary Ti–ZrO_2," *J. Am. Ceram. Soc.*, **56** [11] 584–7 (1973).
[21]R. J. Ackermann, S. P. Garg, and E. G. Rauh, "High-Temperature Phase Diagram for the System Zr–O," *J. Am. Ceram. Soc.*, **60** [7–8] 341–5 (1977). □